Parkinsonism and Related Disorders 67 (2019) 36–41

Contents lists available at ScienceDirect

Parkinsonism and Related Disorders

journal homepage: www.elsevier.com/locate/parkreldis

Altered brain structural topological properties in Parkinson's disease with levodopa-induced dyskinesias

Lina Wang[a,1], Min Wang[b,1], Qianqian Si[a,1], Yongsheng Yuan[a], Kewei Ma[a], Caiting Gan[a], Kezhong Zhang[a,*]

[a] Department of Neurology, The First Affiliated Hospital of Nanjing Medical University, Nanjing, China
[b] Department of Radiology, The First Affiliated Hospital of Nanjing Medical University, Nanjing, China

ARTICLE INFO

Keywords:
Levodopa-induced dyskinesias
Diffusion tensor imaging
Structural network
Topology
Basal ganglia-thalamocortical

ABSTRACT

Objectives: In this study, the alterations of structural topological properties in Parkinson's disease (PD) patients with levodopa-induced dyskinesias (LIDs) were explored using white matter structural network connectome derived from diffusion tensor imaging (DTI).

Methods: 21 dyskinetic PD patients, 21 non-dyskinetic PD patients and 25 healthy controls were studied in global and nodal topological properties of structural networks after controlling age, gender and education. Afterwards, post hoc analyses were performed to explore further differences. Finally, multiple linear regression analysis was employed to test the associations between significant different properties and the severity of dyskinesias in PD.

Results: Dyskinetic PD patients exhibited significant increased global efficiency, local efficiency, clustering coefficient, but decreased shortest path length compared with the non-dyskinetic. Additionally, increased nodal efficiency in bilateral inferior frontal gyrus (IFG), right putamen, right thalamus, and decreased nodal shortest path length in bilateral IFG and right thalamus, were discovered in dyskinetic PD in comparison with non-dyskinetic PD. Notably, a negative correlation between the Abnormal Involuntary Movement Scale (AIMS) scores and shortest path length of whole-brain network was found in PD with LIDs.

Conclusions: Our results indicated excessively optimized topological organization of whole-brain structural connectome in PD patients with LIDs. These findings also illustrated that excessively strengthened basal ganglia-thalamocortical nodal structural connections played an important role in the presence of LIDs.

1. Introduction

Levodopa-induced dyskinesias (LIDs) represent abnormal involuntary movements that occur in about 40% of patients with Parkinson's disease (PD) after 4–6 years of levodopa therapy [1]. Although the pathophysiological mechanisms underlying LIDs are still obscure now, numerous multimodal imaging studies have been applied to explore their possible pathogenesis. Abnormal overactivity of the striatum as well as prefrontal and related lobes, especially the putamen and inferior frontal gyrus (IFG), has been demonstrated to be involved in the development of LIDs [2,3]. Moreover, LIDs were characterized by significant increased gray matter (GM) volume and cortical thickness of inferior frontal cortex compared with PD patients without dyskinesias [4,5]. Although these neuroimaging studies have suggested that altered GM volume, cortical thickness or functional activity of basal ganglia-thalamocortical pathways contributes to the emergence of LIDs in PD, the structural plasticity of brain connectivity and topological changes of the whole-brain connectome correlated with these motor complications remain unknown.

Recent researches indicated that the human brain could be modeled as a network, referred to as a connectome [6], and that it exhibited nontrivial topological principles, such as small-world properties [7]. Brain connectivity datasets consist of networks constructed by brain nodes and connected by anatomical tracts or functional temporal correlations [8]. Complex network analysis has potential to reliably quantify brain networks with a small amount of neurobiologically meaningful and easily computable measures [9]. Recently, white matter (WM) structural network connectome derived from diffusion tensor imaging (DTI) has been increasingly applied to reveal alterations of structural topological properties with graph theory in multiple

* Corresponding author. Department of Neurology, The First Affiliated Hospital of Nanjing Medical University, No. 300 Guangzhou Road, Nanjing, 210029, China.
E-mail address: kezhong_zhang1969@126.com (K. Zhang).
[1] These first three authors contributed equally to this research.

https://doi.org/10.1016/j.parkreldis.2019.09.022
Received 15 July 2019; Received in revised form 26 August 2019; Accepted 18 September 2019

studies [7,10]. Particularly, impaired topological architecture of WM structural connectome was found in PD patients [7,11]. Nevertheless, the alterations of structural topological properties in PD with LIDs are rarely investigated up to now. Therefore, we employed this study to explore the WM structural network alterations in PD patients with LIDs, which might offer us new and deeper insights into neuropathological mechanisms underlying LIDs.

2. Materials and methods

2.1. Subjects

Our study population consisted of 21 dyskinetic PD patients, 21 non-dyskinetic PD patients, and 25 healthy controls. All patients were recruited from the Neurology Unit of the First Affiliated Hospital of Nanjing Medical University and first clinically evaluated by Kezhong Zhang, a neurologist expert in movement disorders, especially in PD. Besides, they were required to fulfill the following criteria: (1) clinical diagnosis of idiopathic PD judging by the UK Parkinson's Disease Society Brain Bank criteria [12]; (2) no family history of PD; (3) a minimum half-year duration of levodopa therapy; (4) presence or absence of peak-dose LIDs after levodopa intake; (5) no contraindications of magnetic resonance imaging (MRI) scans; (6) no evidence of brain anatomical abnormalities; (7) no evidence of global cognitive impairment (Mini-mental State Examination (MMSE) score > 24) [13]; (8) no intake of sedative and hypnotic medications. Particularly, the dyskinetic PD patients involved in our study were all peak-dose LIDs rather than off-period LIDs or diphasic LIDs.

Before MRI examinations, PD individuals underwent face-to-face interviews and clinical assessments, including Hoehn and Yahr (H&Y) stage [14] and Unified Parkinson's Disease Rating Scale section III (UPDRS-III) [15]. MMSE was assessed to exclude cognitive impairment. Total levodopa equivalent daily dose (LEDD) was calculated for each PD participant [16]. Afterwards, PD patients received MRI scans. Finally, each dyskinetic PD subject underwent an Abnormal Involuntary Movement Scale (AIMS) [17] evaluation when developing LIDs following a levodopa intake.

MRI scans were performed at least 12 h after withdrawal from drugs for all PD participants. Meanwhile, twenty-five healthy volunteers with no previous histories of neurological or psychiatric diseases and with normal brain MRIs were matched for age, gender and education with PD patients. All participants gave written informed consent, which was approved by the Ethical Committee of the First Affiliated Hospital of Nanjing Medical University, according to the Helsinki Declaration.

2.2. Acquisition of MRI data

Brain MRI was performed using a 3.0 T S MAGNETOM Verio whole-body MRI system (Siemens Medical Solutions, Germany) with eight-channel, phase-array head coils. Whole-brain T1-weighted anatomical images were acquired using the following volumetric 3D magnetization-prepared rapid gradient-echo (MP-RAGE) sequence. Parameters were as follows: repetition time (TR) = 1900 ms, echo time (TE) = 2.95 ms, flip angle = 9°, slice thickness = 1 mm, slices = 160, field of view (FOV) = 230 × 230 mm^2, matrix size = 256 × 256 and voxel size = 1 × 1 × 1 mm^3. In addition, DTI images were obtained using spin echo planar imaging sequence. Parameters were as follows: TR = 9800 ms, TE = 95 ms, FOV = 256 × 256 mm^2, number of excitations (NEX) = 1, matrix = 128 × 128, slice thickness = 2 mm and slice gap = 0 mm. Diffusion gradients were applied in 30 non-collinear directions with a b factor of 1000 s/mm^2 after an acquisition without diffusion weighting (b = 0 s/mm^2) for reference.

2.3. Image preprocessing and structural network construction

DTI data preprocessing steps included brain extraction, realignment, eddy current and motion artifact correction, fractional anisotropy (FA) calculation, and diffusion tensor tractography. All these steps were performed using the PANDA toolbox (https://www.nitrc.org/projects/panda) based on FMRIB Software Library (FSL 5.0; https://www.nitrc.org/projects/fsl). Deterministic fiber tracking was applied to construct WM structural brain networks. The fiber tracking was performed using Continuous Tracking (FACT) algorithm [18]. The FA threshold was set to 0.2, and the turning angle threshold was set to 45°for the fiber assignment. The quality controls and analyses of magnetic resonance images were performed by an experienced imaging scientist (Min Wang, with 10 years of experience in MRI data analysis).

Each brain was parcellated into 90 regions of interest (ROIs) using Anatomical Automatic Labeling (AAL) atlas, which were defined as 90 nodes used to construct WM structural networks. The parcellation process was performed in the native space. Actually, T1-weighted images of each participant were firstly registered with their corresponding b = 0 image with an affine transformation. Afterwards, the individual transformed T1-weighted images were registered to the ICBM152 T1 template (Montreal Neurological Institute, Montreal, Canada) by a non-linear transformation. Finally, the inversed transformation parameter of each individual was applied to the AAL atlas to generate corresponding AAL regions in individual space. Each AAL region was considered as a node, and interconnections between brain regions were considered as the edges of the structural network.

Interconnections between brain nodes were considered to exist if the number of interconnected WM fibers was > 10 [19], to reduce the signal noise ratio and fake connections. Finally, a symmetric 90 × 90 connectivity matrix for each individual was obtained.

2.4. Network parameter calculation

Graph theoretical analysis was performed on the interregional connectivity matrix by using GRETNA (https://www.nitrc.org/projects/gretna), a graph theoretical network analysis toolbox for imaging connectome. A number of topological properties were calculated for WM structural networks, containing global (including global efficiency (Eg), local efficiency (Eloc), shortest path length (Lp), clustering coefficient (Cp), and small-world index (σ)) and nodal (including nodal efficiency (Ne), nodal clustering coefficient (NCp), nodal local efficiency (NLe), and nodal shortest path length (NLp)) graph parameters.

2.5. Statistical analysis

Demographic and clinical characteristics of all participants in different groups were compared by Chi-square test, one-way analysis of variance (ANOVA), two-sample t-test, Kruskal-Wallis test, or Mann-Whitney test, as appropriate. Significance level was set at $p < 0.05$. All the above analyses were performed with SPSS 20.0 statistical analysis software (SPSS Inc. Chicago, IL, USA).

The significance of inter-group differences in global and nodal properties was firstly analyzed by one-way factorial analysis of covariance (ANCOVA: dyskinetic PD, non-dyskinetic PD and controls) after controlling age, gender and education. For global parameters, $P < 0.05$ was considered significant; for nodal parameters, multiple comparison correction was conducted and false discovery rate (FDR) corrected < 0.05 was considered significant. Hereafter, post hoc analyses were performed to explore further between-group differences. It was worth noting that for post hoc analyses of significant nodal properties, two-sample t tests were applied within these significant brain nodes obtained by the previous one-way ANCOVA analysis. Meanwhile, FDR correction was also conducted due to multiple comparisons. All the graph theoretical parameters analyses were performed with the statistical model of GRETNA.

Finally, multiple linear regression analysis was employed to examine the associations between significant different properties of

Table 1
Demographic and clinical characteristics in PD patients and controls.

Variables	Dyskinetic	Non-dyskinetic	Controls	*P* values
n	21	21	25	NA
Gender (F/M)	8/13	7/14	8/17	0.904[a]
Age (y)	60.33 ± 9.00	63.19 ± 7.28	62.88 ± 5.56	0.379[b]
Education (y)	9.90 ± 4.00	10.48 ± 3.44	11.48 ± 2.97	0.301[c]
Age at onset (y)	50.57 ± 9.91	58.14 ± 7.58	NA	0.008[d], *
Disease duration (y)	9.00 ± 4.17	5.95 ± 2.04	NA	0.016[e], *
H&Y stage	2.52 ± 0.58	2.18 ± 0.77	NA	0.088[e]
UPDRS-III	35.67 ± 14.88	34.38 ± 16.72	NA	0.794[d]
LEDD	745.24 ± 315.15	718.34 ± 332.00	NA	0.870[e]
MMSE	27.90 ± 1.67	28.10 ± 1.09	28.60 ± 1.15	0.352[c]
AIMS	9.16 ± 4.03	NA	NA	NA

Data are presented as mean values ± SD.
Abbreviations: PD: Parkinson's disease; NA: not applicable; F: Female; M: Male; y: year; H&Y: Hoehn and Yahr stage; UPDRS: Unified Parkinson's disease rating scale; LEDD: Levodopa equivalent daily dose; MMSE: Mini Mental State Examination; AIMS: Abnormal Involuntary Movement Scale.
*$P < 0.05$ was set significant.
[a] Chi square test.
[b] One-way analysis of variance.
[c] Kruskal-Wallis test.
[d] Two-sample *t*-test.
[e] Mann-Whitney test.

structural networks and the severity of dyskinesias in PD patients.

3. Results

3.1. Demographics

The demographic and clinical characteristics of all participants were presented in Table 1. No significant differences were found in gender, age and education among the three groups. MMSE scores > 24 were observed in all three groups. Furthermore, the dyskinetic and non-dyskinetic PD patients showed similar H&Y stage, UPDRS-III and LEDD scores. However, PD patients with dyskinesias had a younger age of onset (P = 0.008) and a longer duration of disease (P = 0.016) compared with those without dyskinesias. Hence, these factors would be included as nuisance variables when comparing dyskinetic and non-dyskinetic PD patients.

3.2. Group differences in global parameters

As Table 2 and Fig. 1 shown, dyskinetic, non-dyskinetic PD patients and controls all presented small-world organization (σ > 1) of WM structural networks. However, no significance was detected in σ among the three groups. Significantly different Eg (F = 7.714; P = 0.001), Eloc (F = 5.645; P = 0.006), Lp (F = 7.729; P = 0.001) and Cp (F = 5.309; P = 0.007) were observed among the three groups with one-way ANCOVA, adjusting for age, gender and education. Furthermore, dyskinetic PD patients exhibited significant increased Eg (t = 3.290; P = 0.002), Eloc (t = 3.487; P = 0.001), Cp (t = 3.397; P = 0.002), but decreased Lp (t = −2.979; P = 0.005) compared with non-dyskinetic PD subjects, adjusting for age, gender, education, age of onset and disease duration. In contrast, decreased Eg (t = −2.680; P = 0.011) and increased Lp (t = 2.700; P = 0.010) were discovered in non-dyskinetic PD patients in comparison with healthy controls, adjusting for age, gender and education. There were no significant global topological properties detected between PD patients with LIDs and healthy controls.

Table 2
One-way ANCOVA of global graph parameters among the three groups.

Global parameters	Dyskinetic	Non-dyskinetic	Controls	*P* values
Eg	0.320 ± 0.024	0.281 ± 0.046	0.312 ± 0.031	0.001*,[a,b]
Eloc	0.411 ± 0.055	0.345 ± 0.075	0.389 ± 0.058	0.006*,[a]
Lp	3.146 ± 0.248	3.671 ± 0.707	3.239 ± 0.336	0.001*,[a,b]
Cp	0.322 ± 0.038	0.277 ± 0.051	0.305 ± 0.039	0.007*,[a]
σ	5.001 ± 0.696	4.884 ± 0.504	4.762 ± 0.653	0.613

Group differences in the global measures of structural networks among the three groups were explored with one-way factorial analysis of covariance (ANCOVA), adjusting for age, gender and education. Afterwards, post hoc analyses were adopted to investigate all possible pair-wise comparisons.
*$P < 0.05$ was set significant for one-way ANCOVA.
Abbreviations: Eg: global efficiency; Eloc: local efficiency; Lp: shortest path length; Cp: clustering coefficient; σ: small-world index; PD: Parkinson's disease.
[a] Dyskinetic vs non-dyskinetic PD: two-sample *t*-test was applied, adjusting for age, gender, education, age at onset and disease duration, and p < 0.017 (0.05/3 [number of pair-comparisons]) was considered significant.
[b] Non-dyskinetic PD vs controls: two-sample *t*-test was adopted, adjusting for age, gender and education, and p < 0.017 (0.05/3 [number of pair-comparisons]) was considered significant.

3.3. Group differences in nodal parameters

For nodal parameters, group differences were observed in Ne (P < 0.05, FDR corrected) and NLp (P < 0.05, FDR corrected), and the significant brain nodes were presented in Table 3. Particularly, increased Ne in right opercular part of IFG, bilateral orbital part of IFG, right putamen, right thalamus, and decreased NLp in bilateral orbital part of IFG and right thalamus were discovered in dyskinetic PD patients in comparison with non-dyskinetic PD patients, adjusting for age, gender, education, age at onset and disease duration (Fig. 2A). In addition, non-dyskinetic PD patients showed decreased Ne in left SMA compared with controls, adjusting for age, gender and education (Fig. 2B). Nevertheless, no significant brain nodes were detected between dyskinetic PD patients and healthy controls.

3.4. Correlations between graph parameters and behaviors

Multiple linear regression analysis revealed that no significant associations between AIMS scores and nodal parameters but a negative correlation (t = −2.38, P = 0.028) between AIMS scores and Lp of whole-brain network were detected in PD patients with LIDs (Fig. 3). These results indicated that the severity of dyskinesias in PD was closely associated with altered shortest path length of whole-brain structural networks rather than the nodal properties of WM networks.

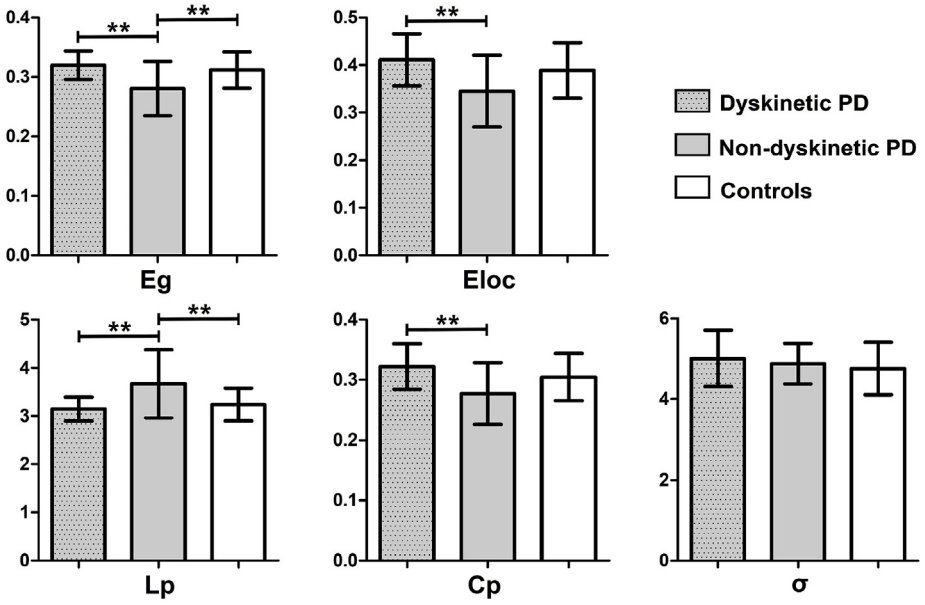

Fig. 1. One-way ANCOVA of global parameters among the three groups.
Significant differences of global parameters of the structural network were detected among the three groups, performed by one-way ANCOVA, adjusting for age, gender and education. $P < 0.05$ was set significant. Afterwards, two-sample *t*-test was employed to explore further differences. Notably, when comparing dyskinetic and non-dyskinetic PD patients, two-sample *t*-test was applied after controlling age, gender, education, age at onset and disease duration. **Post hoc tests were corrected by Bonferroni correction with a significant different $p < 0.017$ (0.05/3 [number of pair-comparisons]). Abbreviations: Eg: global efficiency; Eloc: local efficiency; Lp: shortest path length; Cp: clustering coefficient; σ: small-world index; PD: Parkinson's disease.

4. Discussion

In this study we evaluated the architecture of WM networks in dyskinetic PD patients, non-dyskinetic PD patients and healthy controls, which presented similar small-world organization. However, dyskinetic PD participants exhibited increased Eg, Eloc, Cp, but decreased Lp in comparison with non-dyskinetic PD individuals. Moreover, significant increased Ne was found in PD patients with LIDs, mainly located in the prefrontal, striatum and thalamus regions. Decreased NLp was also observed in dyskinetic PD patients, located in bilateral IFG and right thalamus. In addition, a significant negative correlation between Lp and AIMS scores was detected in PD with LIDs.

Regarding the global topological properties, the small-world architecture is one of the major organizational principles of the complex human brain [9]. The present findings showed a typical small-world topology in controls, and PD patients with or without LIDs, which indicated a conserved small-world architecture in PD, consistent with previous studies [11,20]. However, different from PD patients without dyskinesias, the dyskinetic PD group exhibited significant increased Eg, Eloc, Cp, but decreased Lp of WM structural networks. Eg and Lp represent the averaged ability of inter-nodal information transformation over the whole brain [21]. The findings of increased Eg and decreased Lp in PD with LIDs might suggest that the inter-nodal organization of the whole brain was excessively optimized in dyskinetic PD patients compared with non-dyskinetic PD individuals. Additionally, Eloc and Cp are usually used to assess the ability of the brain to locally handle information [9]. Taken together, PD patients with dyskinesias showed relatively higher ability of the brain to both globally integrate and locally handle information compared to those without dyskinesias. Although the altered structural and functional topological properties in PD with LIDs were few investigated previously, LIDs were considered as the consequence of an abnormal pattern or code of activity. It originated from the basal ganglia and was conveyed to the thalamus and the cortical motor areas, leading to overactivation of cortical motor and premotor areas [2,22]. Therefore, the excessively strengthened capacity of information transferring and processing of the whole brain observed in PD with LIDs might contribute to their hyperkinetic aberrant involuntary movements. Consistent with the hypothesis, our further regression analysis revealed a negative association between Lp and AIMS scores in PD with LIDs. The AIMS has been widely applied to evaluate the severity of abnormal involuntary movements occurred in LIDs [23]. Thence, our results indicated that the excessively optimized WM structural connections of whole brain might provide a structural basis for understanding LIDs in PD patients.

Furthermore, significant increased Ne was discovered in PD patients with LIDs, mainly located in basal ganglia-thalamocortical motor pathways (especially for putamen, thalamus, and IFG), whereas decreased NLp was detected in bilateral IFG and right thalamus in

Table 3
One-way ANCOVA of nodal graph parameters among the three groups.

Brian regions (AAL)	Dyskinetic	Non-dyskinetic	Controls	F values	*P* values
Nodal efficiency					
Frontal_Inf_Oper_R	0.337 ± 0.044	0.295 ± 0.046	0.333 ± 0.044	5.304	0.008
Frontal_Inf_Orb_L	0.333 ± 0.033	0.281 ± 0.047	0.314 ± 0.046	8.647	< 0.001
Frontal_Inf_Orb_R	0.348 ± 0.039	0.302 ± 0.056	0.340 ± 0.041	5.909	0.005
Supp_Motor_Area_L	0.374 ± 0.039	0.335 ± 0.043	0.381 ± 0.032	8.975	< 0.001
Putamen_R	0.414 ± 0.031	0.374 ± 0.050	0.409 ± 0.039	6.266	0.003
Thalamus_R	0.360 ± 0.045	0.297 ± 0.052	0.339 ± 0.033	11.121	< 0.001
Nodal shortest path length					
Frontal_Inf_Orb_L	3.035 ± 0.317	3.687 ± 0.819	3.258 ± 0.539	7.070	0.002
Frontal_Inf_Orb_R	2.918 ± 0.378	3.427 ± 0.679	2.984 ± 0.378	6.537	0.003
Thalamus_R	2.827 ± 0.380	3.465 ± 0.636	2.981 ± 0.316	11.115	< 0.001

Unless indicated otherwise, data were given as the mean ± SD.
One-way factorial analysis of covariance (ANCOVA) was applied to investigate nodal efficiency and nodal shortest path length of the structural networks among the three groups, adjusting for age, gender and education. $P < 0.05$ (false discovery rate corrected) indicated a significant group difference.
Abbreviations: AAL: Anatomical automatic labeling; R: right; L: left.

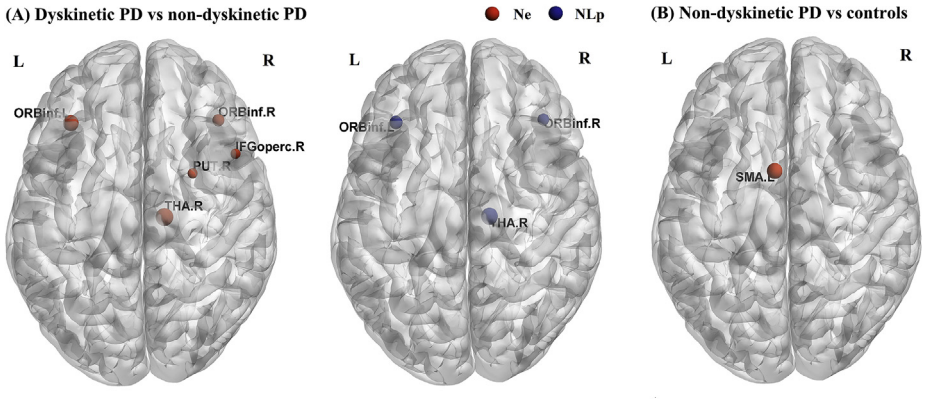

Fig. 2. Between-group comparisons of significant different nodal parameters between all possible pair-wise comparisons.
A: Dyskinetic PD patients showed increased Ne (**red**) in IFGoperc.R, bilateral ORBinf, PUT.R, THA.R and decreased NLp (**blue**) in bilateral ORBinf and THA.R compared with non-dyskinetic PD subjects, after controlling age, gender, education, age at onset and disease duration; B: Compared to controls, decreased Ne (**red**) was found in left SMA in non-dyskinetic PD patients, after controlling age, gender and education. However, there were no significant brain nodes detected between dyskinetic PD patients and controls. These between-group comparisons were corrected by multiple comparison correction and false discovery rate (FDR) corrected < 0.05 was considered significant. The size of the far point indicated the relative T values from two-sample *t*-test. Abbreviations: PD: Parkinson's disease; Ne: nodal efficiency; NLp: nodal shortest path length; IFGoperc: opercular part of inferior frontal gyrus; ORBinf: orbital part of inferior frontal gyrus; PUT: putamen; THA: thalamus; SMA: supplementary motor area; L: left; R: right. (For interpretation of the references to colour in this figure legend, the reader is referred to the Web version of this article.)

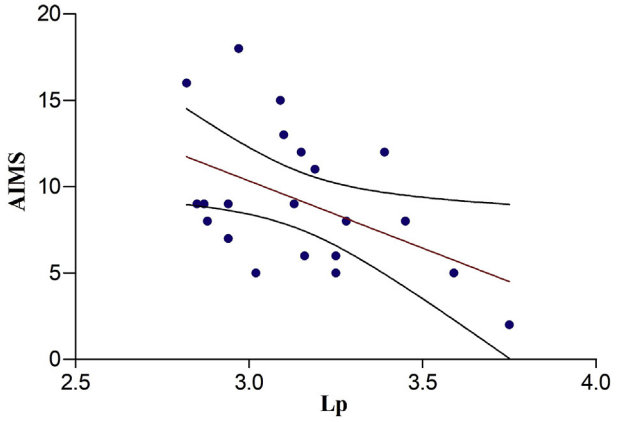

Fig. 3. Correlation between significant graph properties and the severity of dyskinesias in dyskinetic PD group.
A negative correlation between Lp of the whole-brain structural network and AIMS scores was found in dyskinetic PD patients. The association was explored by multiple linear regression, and the regression line (**red**) and the 95% confidence intervals (**black lines**) were shown. P < 0.05 was set significant. Abbreviations: PD: Parkinson's disease; AIMS: Abnormal Involuntary Movement Scale; Lp: shortest path length. (For interpretation of the references to colour in this figure legend, the reader is referred to the Web version of this article.)

dyskinetic PD subjects. Ne and NLp represent the ability of information transfer from a node to other nodes in the entire network [24]. Within the basal ganglia, excessive activation in PD patients with dyskinesias was mainly restricted to the bilateral putamen [2]. This part of the basal ganglia was most strongly affected by dopaminergic denervation in PD [25] and was thought to play a central role in the pathophysiology of dyskinesias [26]. Such a discovery was in good agreement with our observation that right putamen exhibited a different WM architecture in PD patients with LIDs compared with PD patients without dyskinesias. The thalamus receives afferents from striatum and projects mainly to the motor cortex and premotor cortex [27]. It is a relay center serving the motor mechanisms. Thus, the increased Ne and decreased NLp of right thalamus in our study suggested its indispensable role in maintaining the high work efficiency of the basal ganglia-thalamocortical motor pathways. Moreover, the disinhibition and overactivity of prefrontal and related motor cortex, especially the IFG, were considered to be involved in the pathophysiological mechanisms underlying LIDs in previous multimodal imaging studies [3,22,23]. Furthermore, the excessively strengthened striato-cortical connections in response to levodopa (especially from putamen to the primary motor cortex) were certified to produce an aberrant reinforcement signal, producing an abnormal motor drive that ultimately triggered involuntary movements in LIDs [28]. In agreement with this, our findings showed that dyskinetic PD patients exhibited increased Ne, located in right opercular part of IFG, bilateral orbital part of IFG, and decreased NLp in bilateral orbital part of IFG compared with non-dyskinetic PD participants. Interestingly, no significant associations between AIMS scores and nodal parameters but a negative correlation between AIMS scores and Lp of whole-brain network were detected in PD patients with LIDs. This might suggest that LIDs in PD were closely relevant to the alterations of whole-brain structural network rather than a single brain node connectivity. Nevertheless, our findings of excessively strengthened basal ganglia-thalamocortical nodal structural connections could provide evidence to illustrate the neuropathological mechanisms underlying LIDs.

In the present study, we also observed that PD patients with LIDs showed a younger age of onset and a longer duration of disease compared with PD patients without dyskinesias, in correspondence with previous epidemiological studies [29]. In order to reduce the nuisance caused by different age of onset and disease duration, these factors were also included as covariates when comparing dyskinetic and non-dyskinetic PD individuals. In addition, it was interesting that we observed altered neurodegenerative patterns between dyskinetic and non-dyskinetic PD patients, but not between dyskinetic PD patients and controls. Consistent with this, previous several structural studies about LIDs also reported similar findings [4,5]. As Cerasa et al. stated, it might be caused by our highly stringent statistical thresholds (FDR < 0.05) or the special pathophysiological mechanisms of LIDs in PD. Even so, our findings seemed to confirm the hypothesis of maladaptive levodopa-induced neuroplasticity in LIDs patients.

However, our study was characterized by some specific limitations. First, this was a cross-sectional investigation instead of a prospective study, so longitudinal studies should be performed in the future. Second, we took the FACT algorithm to estimate inter-regional structural connectivity, which couldn't resolve complex fiber configurations, such as crossing, kissing, or merged fiber bundles. Therefore, some advanced algorithms or imaging sequences, including a probabilistic tractography algorithm and diffusion spectrum imaging (DSI) technique, were introduced to resolve the question of complex fiber configurations for accurately measuring the fiber tracking. Finally, we only explored WM structural networks in the present study. In future studies, the combination of the multimodal imaging (e.g., structural and functional MRI) would yield a comprehensive understanding of the relationship between structural and functional changes in LIDs.

5. Conclusion

By using diffusion tensor imaging tractography combined with graph analysis, our study found excessively optimized topological organization of whole-brain structural connectome in PD patients with LIDs. These findings also provided evidence that excessively strengthened basal ganglia-thalamocortical nodal structural connections played an important role in the presence of LIDs.

Conflicts of interest

The authors declare there are no competing interests.

Acknowledgment

Funding: This work was supported by the National Natural Science Foundation of China (No. 81671258), the Science and Technology Project of Jiangsu Provincial Commission of Health and Family Planning (No. H201602), the Natural Science Foundation of Jiangsu Province (No. BK20141494), and the National Natural Science Foundation of China (No. 81901297).

References

[1] J.E. Ahlskog, M.D. Muenter, Frequency of levodopa-related dyskinesias and motor fluctuations as estimated from the cumulative literature, Mov. Disord. 16 (2001) 448–458.
[2] D.M. Herz, B.N. Haagensen, M.S. Christensen, K.H. Madsen, J.B. Rowe, A. Lokkegaard, et al., The acute brain response to levodopa heralds dyskinesias in Parkinson disease, Ann. Neurol. 75 (2014) 829–836.
[3] A. Cerasa, G. Koch, G. Donzuso, G. Mangone, M. Morelli, L. Brusa, et al., A network centred on the inferior frontal cortex is critically involved in levodopa-induced dyskinesias, Brain 138 (2015) 414–427.
[4] A. Cerasa, M. Morelli, A. Augimeri, M. Salsone, F. Novellino, M.C. Gioia, et al., Prefrontal thickening in PD with levodopa-induced dyskinesias: new evidence from cortical thickness measurement, Park. Relat. Disord. 19 (2013) 123–125.
[5] A. Cerasa, D. Messina, P. Pugliese, M. Morelli, P. Lanza, M. Salsone, et al., Increased prefrontal volume in PD with levodopa-induced dyskinesias: a voxel-based morphometry study, Mov. Disord. 26 (2011) 807–812.
[6] O. Sporns, G. Tononi, R. Kotter, The human connectome: a structural description of the human brain, PLoS Comput. Biol. 1 (2005) e42.
[7] J.B. Pereira, D. Aarsland, C.E. Ginestet, A.V. Lebedev, L.O. Wahlund, A. Simmons, et al., Aberrant cerebral network topology and mild cognitive impairment in early Parkinson's disease, Hum. Brain Mapp. 36 (2015) 2980–2995.
[8] Y. Chen, K. Chen, J. Zhang, X. Li, N. Shu, J. Wang, et al., Disrupted functional and structural networks in cognitively normal elderly subjects with the APOE varepsilon 4 allele, NEUROPSYCHOPHARMACONeuropsychopharmacologyL 40 (2015) 1181–1191.
[9] E. Bullmore, O. Sporns, Complex brain networks: graph theoretical analysis of structural and functional systems, Nat. Rev. Neurosci. 10 (2009) 186–198.
[10] Y. Zhang, Y. Cao, Y. Xie, L. Liu, W. Qin, S. Lu, et al., Altered brain structural topological properties in type 2 diabetes mellitus patients without complications, J. Diabetes 11 (2019) 129–138.
[11] C. Li, B. Huang, R. Zhang, Q. Ma, W. Yang, L. Wang, et al., Impaired topological architecture of brain structural networks in idiopathic Parkinson's disease: a DTI study, BRAIBrain. Imag. Behav.N IMAGING BEHAV 11 (2017) 113–128.
[12] A.J. Hughes, S.E. Daniel, L. Kilford, A.J. Lees, Accuracy of clinical diagnosis of idiopathic Parkinson's disease: a clinico-pathological study of 100 cases, J. Neurol. Neurosurg. Psychiatry 55 (1992) 181–184.
[13] R.M. Crum, J.C. Anthony, S.S. Bassett, M.F. Folstein, Population-based norms for the Mini-Mental State Examination by age and educational level, J. Am. Med. Assoc. 269 (1993) 2386–2391.
[14] M.M. Hoehn, M.D. Yahr, Parkinsonism: onset, progression and mortality, Neurology 17 (1967) 427–442.
[15] G. Christopher, W.P.O.R. Goetz, The Unified Parkinson's disease rating scale (UPDRS): status and recommendations, Mov. Disord. 18 (2003) 738–750.
[16] C.L. Tomlinson, R. Stowe, S. Patel, C. Rick, R. Gray, C.E. Clarke, Systematic review of levodopa dose equivalency reporting in Parkinson's disease, Mov. Disord. 25 (2010) 2649–2653.
[17] P.R. May, M.A. Lee, R.C. Bacon, Quantitative assessment of neuroleptic-induced extrapyramidal symptoms: clinical and nonclinical approaches, Clin. Neuropharmacol. 6 (Suppl 1) (1983) S35–S51.
[18] S. Mori, P.C. van Zijl, Fiber tracking: principles and strategies - a technical review, NMR Biomed. 15 (2002) 468–480.
[19] N. Shu, X. Wang, Q. Bi, T. Zhao, Y. Han, Disrupted topologic efficiency of white matter structural connectome in individuals with subjective cognitive decline, Radiology 286 (2018) 229–238.
[20] J.M. Hall, J.M. Shine, M.K. Ehgoetz, M. Gilat, K.M. Broadhouse, J. Szeto, et al., Alterations in white matter network topology contribute to freezing of gait in Parkinson's disease, J. Neurol. 265 (2018) 1353–1364.
[21] E. Bullmore, O. Sporns, The economy of brain network organization, Nat. Rev. Neurosci. 13 (2012) 336–349.
[22] O. Rascol, U. Sabatini, C. Brefel, N. Fabre, S. Rai, J.M. Senard, et al., Cortical motor overactivation in parkinsonian patients with L-dopa-induced peak-dose dyskinesia, Brain 121 (Pt 3) (1998) 527–533.
[23] A. Cerasa, M. Salsone, M. Morelli, P. Pugliese, G. Arabia, C.M. Gioia, et al., Age at onset influences neurodegenerative processes underlying PD with levodopa-induced dyskinesias, Park. Relat. Disord. 19 (2013) 883–888.
[24] S. Achard, E. Bullmore, Efficiency and cost of economical brain functional networks, PLoS Comput. Biol. 3 (2007) e17.
[25] S.J. Kish, K. Shannak, O. Hornykiewicz, Uneven pattern of dopamine loss in the striatum of patients with idiopathic Parkinson's disease. Pathophysiologic and clinical implications, N. Engl. J. Med. 318 (1988) 876–880.
[26] M.A. Cenci, M. Lundblad, Post- versus presynaptic plasticity in L-DOPA-induced dyskinesia, J. Neurochem. 99 (2006) 381–392.
[27] M.T. Herrero, C. Barcia, J.M. Navarro, Functional anatomy of thalamus and basal ganglia, Childs Nerv SChild's Nerv. Syst.yst 18 (2002) 386–404.
[28] D.M. Herz, B.N. Haagensen, M.S. Christensen, K.H. Madsen, J.B. Rowe, A. Lokkegaard, et al., Abnormal dopaminergic modulation of striato-cortical networks underlies levodopa-induced dyskinesias in humans, Brain 138 (2015) 1658–1666.
[29] T.N. Tran, T. Vo, K. Frei, D.D. Truong, Levodopa-induced dyskinesia: clinical features, incidence, and risk factors, J. Neural Transm. 125 (2018) 1109–1117.